

## Mechanistic Study of Precursor Evolution in Colloidal Group II–VI Semiconductor Nanocrystal Synthesis

Haitao Liu, Jonathan S. Owen, and A. Paul Alivisatos\*

Contribution from the Department of Chemistry, University of California, and Materials Science Division, Lawrence Berkeley National Laboratory, Berkeley, California 94720

Received August 4, 2006; E-mail: alivis@uclink.berkeley.edu

**Abstract:** The molecular mechanism of precursor evolution in the synthesis of colloidal group II–VI semiconductor nanocrystals was studied using  $^1\text{H}$ ,  $^{13}\text{C}$ , and  $^{31}\text{P}$  NMR spectroscopy and mass spectrometry. Tri-*n*-butylphosphine chalcogenides (TBPE; E = S, Se, Te) react with an oleic acid complex of cadmium or zinc (M–OA; M = Zn, Cd) in a noncoordinating solvent (octadecene (ODE), *n*-nonane- $d_{20}$ , or *n*-decane- $d_{22}$ ), affording ME nanocrystals, tri-*n*-butylphosphine oxide (TBPO), and oleic acid anhydride ((OA) $_2$ O). Likewise, the reaction between trialkylphosphine selenide and cadmium *n*-octadecylphosphonic acid complex (Cd–ODPA) in tri-*n*-octylphosphine oxide (TOPO) produces CdSe nanocrystals, trialkylphosphine oxide, and anhydrides of *n*-octadecylphosphonic acid. The disappearance of tri-*n*-octylphosphine selenide in the presence of Cd–OA and Cd–ODPA can be fit to a single-exponential decay ( $k_{\text{obs}} = (1.30 \pm 0.08) \times 10^{-3} \text{ s}^{-1}$ , Cd–ODPA, 260 °C, and  $k_{\text{obs}} = (1.51 \pm 0.04) \times 10^{-3} \text{ s}^{-1}$ , Cd–OA, 117 °C). The reaction approaches completion at 70–80% conversion of TOPSe under anhydrous conditions and 100% conversion in the presence of added water. Activation parameters for the reaction between TBPSe and Cd–OA in *n*-nonane- $d_{20}$  were determined from the temperature dependence of the TBPSe decay over the range of 358–400 K ( $\Delta H^\ddagger = 62.0 \pm 2.8 \text{ kJ}\cdot\text{mol}^{-1}$ ,  $\Delta S^\ddagger = -145 \pm 8 \text{ J}\cdot\text{mol}^{-1}\cdot\text{K}^{-1}$ ). A reaction mechanism is proposed where trialkylphosphine chalcogenides deoxygenate the oleic acid or phosphonic acid surfactant to generate trialkylphosphine oxide and oleic or phosphonic acid anhydride products. Results from kinetics experiments suggest that cleavage of the phosphorus chalcogenide double bond (TOP=E) proceeds by the nucleophilic attack of phosphonate or oleate on a (TOP=E)–M complex, generating the initial M–E bond.

### Introduction

The synthesis of group II–VI colloidal nanocrystals by thermal decomposition of organometallic precursors has been extensively used in the past decade. This synthetic approach was first reported for the synthesis of cadmium chalcogenide quantum dots,<sup>1</sup> nanorods,<sup>2,3</sup> and tetrapods<sup>3,4</sup> in tri-*n*-octylphosphine oxide (TOPO) using CdMe<sub>2</sub> and tri-*n*-octylphosphine selenide (TOPSe) as precursors. Later, a more synthetically convenient precursor, CdO,<sup>5,6</sup> was introduced to replace CdMe<sub>2</sub>, and noncoordinating solvents, such as octadecene (ODE), were used to replace TOPO.<sup>7</sup> Besides its application in the syntheses of quantum dots, rods, and tetrapods of cadmium chalcogenides, this thermal decomposition method has also been extended to the synthesis of ZnS and ZnSe nanocrystals<sup>8</sup> as well as core–shell dots and rods,<sup>9,10</sup> branched rods and tetrapods,<sup>11,12</sup> and

quantum dot–quantum well structures.<sup>13,14</sup> The quality and control over nanocrystals prepared using these methods have made them key pieces in the development of fluorescent labels,<sup>15–17</sup> light-emitting diodes,<sup>18,19</sup> solar cells,<sup>20–22</sup> and other electronic devices.<sup>23</sup>

- (1) Murray, C. B.; Norris, D. J.; Bawendi, M. G. *J. Am. Chem. Soc.* **1993**, *115*, 8706–8715.
- (2) Peng, X. G.; Manna, L.; Yang, W. D.; Wickham, J.; Scher, E.; Kadavanich, A.; Alivisatos, A. P. *Nature* **2000**, *404*, 59–61.
- (3) Manna, L.; Scher, E. C.; Alivisatos, A. P. *J. Am. Chem. Soc.* **2000**, *122*, 12700–12706.
- (4) Manna, L.; Milliron, D. J.; Meisel, A.; Scher, E. C.; Alivisatos, A. P. *Nat. Mater.* **2003**, *2*, 382–385.
- (5) Peng, Z. A.; Peng, X. G. *J. Am. Chem. Soc.* **2001**, *123*, 183–184.
- (6) Qu, L. H.; Peng, Z. A.; Peng, X. G. *Nano Lett.* **2001**, *1*, 333–337.
- (7) Yu, W. W.; Peng, X. G. *Angew. Chem., Int. Ed.* **2002**, *41*, 2368–2371.
- (8) Lin, S. L.; Pradhan, N.; Wang, Y. J.; Peng, X. G. *Nano Lett.* **2004**, *4*, 2261–2264.

- (9) Manna, L.; Scher, E. C.; Li, L. S.; Alivisatos, A. P. *J. Am. Chem. Soc.* **2002**, *124*, 7136–7145.
- (10) Peng, X. G.; Schlamp, M. C.; Kadavanich, A. V.; Alivisatos, A. P. *J. Am. Chem. Soc.* **1997**, *119*, 7019–7029.
- (11) Milliron, D. J.; Hughes, S. M.; Cui, Y.; Manna, L.; Li, J. B.; Wang, L. W.; Alivisatos, A. P. *Nature* **2004**, *430*, 190–195.
- (12) Kanaras, A. G.; Sonnichsen, C.; Liu, H. T.; Alivisatos, A. P. *Nano Lett.* **2005**, *5*, 2164–2167.
- (13) Battaglia, D.; Li, J. J.; Wang, Y. J.; Peng, X. G. *Angew. Chem., Int. Ed.* **2003**, *42*, 5035–5039.
- (14) Battaglia, D.; Blackman, B.; Peng, X. G. *J. Am. Chem. Soc.* **2005**, *127*, 10889–10897.
- (15) Bruchez, M.; Moronne, M.; Gin, P.; Weiss, S.; Alivisatos, A. P. *Science* **1998**, *281*, 2013–2016.
- (16) Alivisatos, P. *Nat. Biotechnol.* **2004**, *22*, 47–52.
- (17) Gerion, D.; Parak, W. J.; Williams, S. C.; Zanchet, D.; Micheel, C. M.; Alivisatos, A. P. *J. Am. Chem. Soc.* **2002**, *124*, 7070–7074.
- (18) Colvin, V. L.; Schlamp, M. C.; Alivisatos, A. P. *Nature* **1994**, *370*, 354–357.
- (19) Coe, S.; Woo, W. K.; Bawendi, M.; Bulovic, V. *Nature* **2002**, *420*, 800–803.
- (20) Huynh, W. U.; Peng, X. G.; Alivisatos, A. P. *Adv. Mater.* **1999**, *11*, 923–927.
- (21) Huynh, W. U.; Dittmer, J. J.; Alivisatos, A. P. *Science* **2002**, *295*, 2425–2427.
- (22) Gur, I.; Fromer, N. A.; Geier, M. L.; Alivisatos, A. P. *Science* **2005**, *310*, 462–465.
- (23) Cui, Y.; Banin, U.; Bjork, M. T.; Alivisatos, A. P. *Nano Lett.* **2005**, *5*, 1519–1523.

The kinetics of growth and shape evolution, especially that of CdSe, has been discussed extensively. Many important concepts such as size distribution focusing,<sup>24</sup> selective adhesion shape control,<sup>2,3,25</sup> and branching<sup>3,4,12</sup> have been developed. Recent kinetic studies by Peng,<sup>26,27</sup> as well as by Mulvaney,<sup>28,29</sup> have examined the nucleation and growth of CdSe quantum dots and rods by monitoring the time-dependent evolution of the nanocrystals. In spite of the important conclusions from these studies, they have yet to be linked to a detailed understanding of how precursor molecules are converted to group II–VI materials.

Using a combination of NMR (<sup>1</sup>H, <sup>13</sup>C, and <sup>31</sup>P) spectroscopy and mass spectrometry (MS), we have investigated the synthesis of group II–VI semiconductor nanocrystals in TOPO and ODE by following the disappearance and appearance of molecular precursors and products. Our results show that surfactant molecules are *reactants* that convert precursor molecules to II–VI semiconductor materials. In particular, our experiments suggest that trialkylphosphine chalcogenides deoxygenate the alkylphosphonate or alkylcarboxylate surfactants, liberating the chalcogen atom. A mechanism is proposed where nucleophiles such as alkylphosphonate and alkylcarboxylate attack a Lewis acid activated (TOP=E)–M (E = S, Se, Te; M = Zn, Cd) complex, breaking the P=E double bond.

## Experimental Section

Tri-*n*-octylphosphine (TOP; 97%, Strem), tri-*n*-butylphosphine (TBP; 99%, Strem), triisopropylphosphine (Aldrich), TOPO (Aldrich, 99%, lot numbers 24801MB and 04017PC),<sup>30</sup> *n*-octadecylphosphonic acid (H<sub>2</sub>–ODPA; Polycarbon), CdO (Aldrich, 99.99+%), ZnO (Aldrich, 99.99+%), oleic acid (H–OA; Aldrich, 99%), *n*-nonane-*d*<sub>20</sub> (Aldrich, 98 atom % D), *n*-decane-*d*<sub>22</sub> (Arcos, 99 atom % D), and ODE (Aldrich, 90%) were used as received. Standard air-sensitive techniques were used to handle air- and moisture-sensitive compounds.

**NMR Methods.** All NMR (<sup>1</sup>H, <sup>13</sup>C, and <sup>31</sup>P) spectra were collected on a 400 MHz Bruker Advance spectrometer. <sup>31</sup>P NMR spectra were acquired either without proton decoupling or with inverse gated decoupling, and care was taken to ensure adequate relaxation ( $\geq 5T_1$ ) between pulses. In situ kinetics experiments were conducted under vacuum in flame-sealed NMR tubes. These samples were inserted into a preheated NMR probe that was calibrated using ethylene glycol as a standard according to an established procedure.<sup>31</sup> CDCl<sub>3</sub> solutions of aliquots from the TOPO-based reaction were prepared in air. Control experiments showed that CDCl<sub>3</sub> solutions of TOPE and TBPE (E = Se, S) stored in air at room temperature are air stable for several weeks, with only <2% conversion to TOPO by <sup>31</sup>P NMR spectroscopy (Figure S2, Supporting Information).

The concentration of phosphine chalcogenide was obtained by comparing the integral of its <sup>31</sup>P NMR peak with that of the phosphine oxide peak and assuming the total concentration of the two species was constant during the reaction. This assumption was verified to be valid (<±2% error) by using an internal standard (ethylphosphonic acid diethyl ester) in the in situ kinetics runs. The <sup>31</sup>P NMR resonances of TOPO and TOPS partially overlap (Figure S3, Supporting Informa-

tion), in which case peak integrals were obtained by deconvolution of the two resonances using MestReC (Mestrelab Research). A detailed discussion of the accuracy of the NMR method used in this study can be found in the Supporting Information.

**Synthesis and Characterization of TOPSe, Tri-*n*-octylphosphine Sulfide (TOPS), Tri-*n*-butylphosphine Sulfide (TBPS), TBPSe, Tri-*n*-butylphosphine Telluride (TBPTe), and Triisopropylphosphine Selenide (*i*-TPPSe).** Traditional syntheses of group II–VI nanocrystals use a mixture of TOP and TOPE (or a mixture of TBP and TBPE) as the injection solution.<sup>27</sup> To simplify the analysis, we used the pure phosphine chalcogenide instead of a mixture with its parent phosphine. Phosphine chalcogenides were prepared by stirring the appropriate phosphine with a stoichiometric or excess amount of elemental S/Se/Te in a glovebox at room temperature. The supernatant was separated from the excess solid chalcogenide and was found to be pure by NMR (<sup>1</sup>H, <sup>13</sup>C, and <sup>31</sup>P) and elemental analysis (Supporting Information).

**Synthesis of Cadmium and Zinc Oleic Acid Complexes (M–OA; M = Zn, Cd).**<sup>32</sup> To a 25 mL flask was added H–OA (4.55 g, 16 mmol) and CdO (0.518 g, 4.0 mmol). The mixture was degassed at 100 °C and 250 mTorr for 30 min. The flask was then filled with Ar and heated to 190 °C to dissolve CdO. After the dissolution of CdO, the mixture was cooled to 110 °C and degassed again at 300 mTorr for 20 min. The solution was then cooled to room temperature and stored in a freezer under N<sub>2</sub>. A stock solution was prepared by dissolving 2.40 g of this complex in 1.60 g of *n*-nonane-*d*<sub>20</sub> and was used in the synthesis of CdS, CdSe, and CdTe. Zn–OA was prepared similarly by dissolving ZnO (0.167 g, 2.05 mmol) in a mixture of H–OA (2.319 g, 8.02 mmol) and ODE (2.50 g) at 300 °C under Ar followed by degassing at 100 °C. The neat reaction mixture was used in the synthesis of ZnS, ZnSe, and ZnTe.

**CdSe Synthesis in TOPO/H<sub>2</sub>–ODPA at 260 °C: “Doubly Degassed” Protocol.** To a 25 mL three-neck flask equipped with a condenser and a thermocouple adapter were added TOPO (2.73 g, 7.06 mmol), H<sub>2</sub>–ODPA (1.07 g, 3.20 mmol), and CdO (0.204 g, 1.60 mmol). The mixture was degassed at 120 °C and 200–400 mTorr pressure for 60 min. The flask was then filled with Ar, and the temperature was raised to 320 °C to dissolve CdO. After CdO was dissolved, the temperature was lowered to 150–180 °C and the pressure was reduced to ~300 mTorr for 60 min (this step will be referred to in the text as the “second degassing”). The flask was then filled with Ar, and the temperature was raised to 270 °C. TOPSe (0.70 g, 1.6 mmol) was injected, and the temperature was allowed to stabilize at 260 ± 2 °C. The amount of TOPSe injected (1.4 ± 0.1 mmol) was measured as the difference between the masses of the syringe before and after the injection. Aliquots taken after the injection of TOPSe were dissolved in CDCl<sub>3</sub> and transferred to NMR tubes in air. NMR spectra of the aliquots were collected within 24 h of sampling.

**In Situ Monitoring of the CdSe Synthesis in *n*-Nonane-*d*<sub>20</sub>.** To a 5 mL NMR tube were added TOPSe (0.0809 g, 0.18 mmol), the Cd–OA stock solution (0.375 g, 0.18 mmol of Cd<sup>2+</sup> and 0.72 mmol of H–OA/OA), and *n*-nonane-*d*<sub>20</sub> (0.0478 g). The mixture was degassed by four freeze–pump–thaw cycles before the NMR tube was flame sealed under vacuum. The NMR probe was then preheated to the desired reaction temperature, and the sample was inserted into the probe and allowed to temperature equilibrate for 4 min before NMR spectra (<sup>1</sup>H, <sup>13</sup>C, and <sup>31</sup>P) were collected. NMR spectra were collected at room temperature before and after the reaction to analyze the reaction products.

Syntheses of other group II–VI materials were carried out similarly using TBPE and M–OA (E = S, Se, Te; M = Zn, Cd) in *n*-nonane-*d*<sub>20</sub>, *n*-decane-*d*<sub>22</sub>, or ODE (Supporting Information).

(24) Peng, X. G.; Wickham, J.; Alivisatos, A. P. *J. Am. Chem. Soc.* **1998**, *120*, 5343–5344.

(25) Peng, Z. A.; Peng, X. G. *J. Am. Chem. Soc.* **2001**, *123*, 1389–1395.

(26) Qu, L. H.; Yu, W. W.; Peng, X. P. *Nano Lett.* **2004**, *4*, 465–469.

(27) Peng, Z. A.; Peng, X. G. *J. Am. Chem. Soc.* **2002**, *124*, 3343–3353.

(28) Bullen, C. R.; Mulvaney, P. *Nano Lett.* **2004**, *4*, 2303–2307.

(29) van Embden, J.; Mulvaney, P. *Langmuir* **2005**, *21*, 10226–10233.

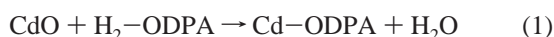
(30) We found that the purity of TOPO is less than 99% on the basis of its <sup>31</sup>P NMR spectrum (Supporting Information Figure S1). The same batch of TOPO was used whenever two experimental results were to be compared.

(31) Ammann, C.; Meier, P.; Merbach, A. E. *J. Magn. Reson.* **1982**, *46*, 319–321.

(32) Yu, W. W.; Wang, Y. A.; Peng, X. G. *Chem. Mater.* **2003**, *15*, 4300–4308.

## Results

**Characterization of Reaction Precursors.** Dissolution of cadmium oxide (CdO) with phosphonic acids has been reported to produce a phosphonic acid complex of cadmium.<sup>5,27</sup> A balanced chemical equation for this reaction is shown in eq 1.



Upon heating cadmium oxide and H<sub>2</sub>-ODPA in TOPO, immiscible, colorless droplets form on the walls of the reaction vessel. <sup>1</sup>H NMR analysis of these droplets in DMSO-*d*<sub>6</sub> showed no peaks other than an increase in the amount of water impurity in the NMR solvent. The moisture content of this reaction mixture was further analyzed using a Karl Fischer titration (see the Supporting Information for experimental details).<sup>33,34</sup> The titration results indicate that both commercial samples of TOPO and H<sub>2</sub>-ODPA used in this study have <0.2% (w/w) moisture. To confirm the stoichiometry of eq 1, CdO (0.211 g, 1.64 mmol) was dissolved in a mixture of TOPO (1.00 g) and H<sub>2</sub>-ODPA (1.07 g, 3.20 mmol) in a tightly closed vial filled with argon at high temperature, and the resulting mixture was cooled and dissolved in anhydrous ethanol in a glovebox. Karl Fischer titration showed that the mixture contained 32 mg of water. After subtraction of the moisture in TOPO and H<sub>2</sub>-ODPA, it was found that 28 mg (1.56 mmol; expected 29.6 mg, 1.64 mmol) of water was produced upon dissolution of the CdO. To test the effectiveness of the second degassing after decomposition of CdO, the reaction mixture was titrated after it had been degassed for 5 min and only 3 mg (0.17 mmol, ~10%) of water remained.

<sup>31</sup>P NMR spectroscopy was also used to characterize the cadmium *n*-octadecylphosphonate complex (Cd-ODPA). Immediately after CdO was dissolved with H<sub>2</sub>-ODPA in TOPO, the mixture was dissolved in CDCl<sub>3</sub>, giving a clear, viscous solution that became turbid after standing for more than a day. <sup>31</sup>P NMR analysis of freshly prepared CDCl<sub>3</sub> solutions of Cd-ODPA showed a sharp TOPO resonance and one broad peak at δ = 25 ppm (fwhm = 10 ppm). No resonances for free H<sub>2</sub>-ODPA were observed. In addition, the acid proton of H<sub>2</sub>-ODPA could not be located in the <sup>1</sup>H NMR spectrum. A similar NMR analysis was performed on the oleic acid complex of cadmium (Cd-OA) prepared by the analogous decomposition of CdO in H-OA using a 4:1 molar ratio of H-OA to CdO. <sup>1</sup>H and <sup>13</sup>C NMR analysis of Cd-OA showed spectra similar to those of H-OA except that the relative intensity of the acidic proton had dropped 50% due to the consumption of 2 equiv of H-OA during the dissolution of CdO. The oleic acid complex of zinc (Zn-OA), on the other hand, was much less soluble in CDCl<sub>3</sub> and was not analyzed.

<sup>31</sup>P NMR chemical shifts of Cd-ODPA, as well as the other phosphorus-containing reagents, dissolved in CDCl<sub>3</sub> are shown in Table 1. H<sub>2</sub>-ODPA is very insoluble in CDCl<sub>3</sub>, and hence, its <sup>31</sup>P NMR spectrum was recorded in methanol-*d*<sub>4</sub>/ethanol (1:3, v/v), showing one resonance at δ = 29.4 ppm. *n*-Tetradecylphosphonic acid (H<sub>2</sub>-TDPA) and *n*-octylphosphonic acid (H<sub>2</sub>-OPA) are, however, more soluble in CDCl<sub>3</sub> and showed singlets at δ = 38.4 and 37.7 ppm, respectively. A solution of

**Table 1.** <sup>31</sup>P NMR Chemical Shifts of the Phosphorus-Containing Surfactants and Precursors<sup>a</sup>

	δ( <sup>31</sup> P) (ppm)	<sup>1</sup> J( <sup>31</sup> P– <sup>77</sup> Se) (Hz)		δ( <sup>31</sup> P) (ppm)	<sup>1</sup> J( <sup>31</sup> P– <sup>77</sup> Se) (Hz)
TOPO	48.5		TBPSe	36.8	680
TOPO + H <sub>2</sub> - ODPA <sup>b</sup>	50.2, 33.7, 24.1		TBPTe	−13.2	1655 <sup>d</sup>
TOPS	48.6		H <sub>2</sub> -OPA	37.7	
TOPSe	36.4	678	H <sub>2</sub> -TDPA	38.4	
TOPSe + Cd <sup>2+</sup> <sup>c</sup>	39.3	615	H <sub>2</sub> -ODPA <sup>e</sup>	29.4	
TBPS	48.7		Cd-ODPA	25	

<sup>a</sup> All spectra were taken in CDCl<sub>3</sub> at room temperature and referenced to the peak for trimethyl phosphate (δ = 3.0 ppm). <sup>b</sup> Prepared by heating H<sub>2</sub>-ODPA and TOPO (1:2, w/w) under Ar to 290 °C and then dissolving the mixture in CDCl<sub>3</sub>. <sup>c</sup> Cadmium 2-ethylhexanoate. <sup>d</sup> <sup>1</sup>J(<sup>31</sup>P–<sup>125</sup>Te). <sup>e</sup> Solvent CD<sub>3</sub>OD/CH<sub>3</sub>CH<sub>2</sub>OH (1:3, v/v).

H<sub>2</sub>-ODPA in CDCl<sub>3</sub> could be obtained by dissolving a hot mixture of H<sub>2</sub>-ODPA and TOPO in CDCl<sub>3</sub> or by heating H<sub>2</sub>-ODPA and TOPO in CDCl<sub>3</sub>. A <sup>31</sup>P NMR spectrum of this mixture (H<sub>2</sub>-ODPA:TOPO = 1:2, w/w) contains three peaks at δ = 50.2 ppm (TOPO), 33.7 ppm (H<sub>2</sub>-ODPA), and 24.1 ppm (Table 1). The resonance at 24.1 ppm does not arise from an impurity of TOPO or ODPa, since it is not observed in a CDCl<sub>3</sub> solution of pure TOPO or in a methanol-*d*<sub>4</sub>/ethanol solution of pure H<sub>2</sub>-ODPA. In addition, the intensity of the 24.1 ppm peak is 8% of the H<sub>2</sub>-ODPA peak intensity in a concentrated sample (50 mg of H<sub>2</sub>-ODPA and 75 mg of TOPO in 1 mL of CDCl<sub>3</sub>) and decreases to <2% in a dilute sample (5 mg of H<sub>2</sub>-ODPA and 10 mg of TOPO in 1 mL of CDCl<sub>3</sub>). This concentration dependence suggests that the 24.1 ppm peak may arise from a hydrogen-bonded complex between TOPO and H<sub>2</sub>-ODPA or between two or more H<sub>2</sub>-ODPA molecules.<sup>35</sup>

The chemical shifts of H<sub>2</sub>-ODPA, TOPO, and TOPSe were found to be sensitive to the presence of Lewis acids and bases. For example, the TOPO resonance shifts downfield from its pure form with added H<sub>2</sub>-ODPA, and the major H<sub>2</sub>-ODPA resonance shifts upfield with added TOPO (Table 1). The chemical shift of TOPSe was also found to be sensitive to the presence of added Lewis acids. Addition of cadmium 2-ethylhexanoate to a CDCl<sub>3</sub> solution of TOPSe caused its <sup>31</sup>P NMR resonance to shift to higher δ and a decrease in <sup>1</sup>J(<sup>31</sup>P–<sup>77</sup>Se) (Table 1). In contrast, however, the addition of cadmium octylphosphonate<sup>36</sup> to TOPSe in CDCl<sub>3</sub> did not change the chemical shift of TOPSe, nor did it affect <sup>1</sup>J(<sup>31</sup>P–<sup>77</sup>Se). In addition, aliquots taken in the CdSe synthesis using TOPSe and Cd-ODPA in TOPO did not show any change in the chemical shift or <sup>1</sup>J(<sup>31</sup>P–<sup>77</sup>Se) of TOPSe when compared to a solution of pure TOPSe in CDCl<sub>3</sub>.

**Characterization of Reaction Products.** In situ <sup>31</sup>P NMR spectroscopy was used to monitor the reaction of Cd-OA or Zn-OA with TBPSe in a hydrocarbon solvent in flame-sealed NMR tubes. In the cases of both Cd and Zn the disappearance of TBPSe proceeds with the formation of TBPO, which was verified by the addition of an authentic sample to the NMR sample as well as by detection with mass spectrometry (Figures 1 and S4, Supporting Information). In several examples, the total concentration of TBPSe and TBPO was constant throughout the reaction (within ±2%), versus an internal standard

(33) Verhoef, J. C.; Barendrecht, E. *J. Electroanal. Chem.* **1977**, *75*, 705–717.

(34) Verhoef, J. C.; Barendrecht, E. *Anal. Chim. Acta* **1977**, *94*, 395–403.

(35) Clearfield, A.; Sharma, C. V. K.; Zhang, B. P. *Chem. Mater.* **2001**, *13*, 3099–3112.

(36) This was prepared by adding CdMe<sub>2</sub> to a CDCl<sub>3</sub> solution of *n*-octylphosphonic acid at room temperature in a glovebox.



**Table 2.** Spectroscopically Characterized Reaction Products from the Synthesis of Group II–VI Nanocrystals<sup>a</sup>

	precursor	surfactant/solvent	identified products (characterization)
CdSe	TBPS <sub>e</sub> /Cd–ODPA	H <sub>2</sub> –ODPA/TOPO	TBPO (FAB-MS)
CdSe	TOPSe/Cd–ODPA	H <sub>2</sub> –ODPA/TOPO	ODPA anhydride ( <sup>31</sup> P NMR, <sup>31</sup> P– <sup>31</sup> P COSY)
CdSe	TBPS <sub>e</sub> /Cd–ODPA	H <sub>2</sub> –ODPA/TOPO, TBP	ODPA anhydride ( <sup>31</sup> P NMR)
CdSe	TBPS <sub>e</sub> /Cd–OA <sup>b</sup>	H–OA/C <sub>10</sub> D <sub>22</sub>	TBPO ( <sup>31</sup> P NMR), (OA) <sub>2</sub> O ( <sup>13</sup> C NMR)
CdSe	TBPS <sub>e</sub> /Cd–OA <sup>b,c</sup>	H–OA/C <sub>10</sub> D <sub>22</sub> , TBP	TBPO ( <sup>31</sup> P NMR), (OA) <sub>2</sub> O ( <sup>13</sup> C NMR)
CdS	TBPS/Cd–OA <sup>b</sup>	H–OA/C <sub>10</sub> D <sub>22</sub>	TBPO ( <sup>31</sup> P NMR, FAB-MS), (OA) <sub>2</sub> O ( <sup>13</sup> C NMR)
CdTe	TBPTe/Cd–OA <sup>b</sup>	H–OA/C <sub>10</sub> D <sub>22</sub>	TBPO ( <sup>31</sup> P NMR), (OA) <sub>2</sub> O ( <sup>13</sup> C NMR)
ZnS	TBPS/Zn–OA <sup>b</sup>	H–OA/ODE	TBPO ( <sup>31</sup> P NMR, FAB-MS), (OA) <sub>2</sub> O ( <sup>13</sup> C NMR)
ZnSe	TBPS <sub>e</sub> /Zn–OA <sup>b</sup>	H–OA/ODE	TBPO ( <sup>31</sup> P NMR, FAB-MS), (OA) <sub>2</sub> O ( <sup>13</sup> C NMR)
ZnTe	TBPTe/Zn–OA <sup>b,d</sup>	H–OA/C <sub>10</sub> D <sub>22</sub> , TBP	TBPO ( <sup>31</sup> P NMR), (OA) <sub>2</sub> O ( <sup>13</sup> C NMR)

<sup>a</sup> The nanocrystal products were characterized by transmission electron microscopy (Figure S8, Supporting Information), UV–vis spectroscopy (Figure S9, Supporting Information), and powder X-ray diffraction. COSY = correlation spectroscopy. C<sub>10</sub>D<sub>22</sub> = *n*-decane-*d*<sub>22</sub>. <sup>b</sup> In a degassed and flame-sealed NMR tube. <sup>c</sup> TBP:TBPS<sub>e</sub> = 1:1 (mol/mol). <sup>d</sup> TBP:TBPTe = 1:1 (w/w).

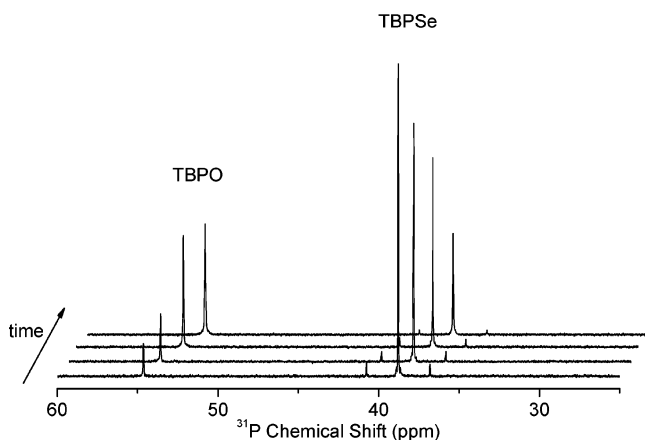


**Figure 1.** Time evolution of the <sup>31</sup>P NMR spectrum of the reaction between TBPS<sub>e</sub> and Cd–OA in *n*-nonane-*d*<sub>20</sub> at 380 K. Spectra were collected at 0, 140, 1110, and 2145 s, respectively.

(ethylphosphonic acid diethyl ester), which requires that TBPO is the only major product of TBPS<sub>e</sub> decomposition. A fast atom bombardment (FAB) mass spectrum of the crude reaction mixture shows a strong peak at *m/z* = 219 corresponding to the [TBPO + H]<sup>+</sup> ion (Figure S4). Similar to the synthesis in hydrocarbon solvents, a synthesis of CdSe, in TOPO solvent using TBPS<sub>e</sub> as the Se precursor, also afforded TBPO as one of the major reaction products. Analysis of a crude reaction mixture using FAB-MS showed a strong peak at *m/z* = 219 that corresponds to the [TBPO + H]<sup>+</sup> ion (Figure S5, Supporting Information).

In addition to the conversion of TBPS<sub>e</sub> to TBPO, the formation of oleic acid anhydride ((OA)<sub>2</sub>O) was observed in the <sup>13</sup>C NMR spectrum of reactions between Zn–OA or Cd–OA and TBPS<sub>e</sub>. In situ analysis of the reaction products showed new peaks at  $\delta$  = 168.1, 129.8, 129.4, and 35.1 ppm not present before the mixture was heated. Comparison of this spectrum with an authentic sample of (OA)<sub>2</sub>O confirmed the assignment (Figure 2).<sup>37</sup> In several runs, the appearance of the  $\alpha$ -methylene peak (<sup>1</sup>H NMR) of (OA)<sub>2</sub>O ( $\delta$  = 2.50 ppm) matches the disappearance of the <sup>31</sup>P NMR resonance of TBPS<sub>e</sub> (within  $\pm$ 2%). Similar observations were made in the synthesis of other metal chalcogenides as well as when the reactions were conducted in the presence of added trialkylphosphine (Table 2, Figure S7, Supporting Information).

(37) Control experiments showed that heating the Cd–OA stock solution (at 120 °C in a degassed and sealed NMR tube for 2 h) or pure H–OA (at 120 °C under a dynamic vacuum for 2 h) did not produce a detectable amount of (OA)<sub>2</sub>O by <sup>1</sup>H and <sup>13</sup>C NMR.

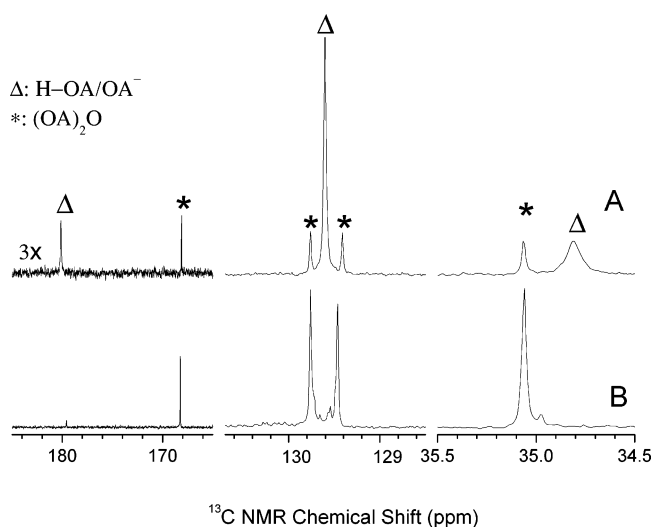


**Figure 2.** <sup>13</sup>C NMR spectrum of (A) the reaction between Cd–OA and TBPS<sub>e</sub> and (B) an authentic sample of (OA)<sub>2</sub>O in *n*-nonane-*d*<sub>20</sub>. (\*) (OA)<sub>2</sub>O peaks: 168.1 ppm, (–CH<sub>2</sub>CO)<sub>2</sub>O; 129.8 and 129.4 ppm, –CH=CH–; 35.1 ppm, (–CH<sub>2</sub>COO)<sub>2</sub>O. (Δ) H–OA peaks: 180.1 ppm, –CH<sub>2</sub>COOH; 129.6 ppm, –CH=CH–; 34.8 ppm, –CH<sub>2</sub>COOH. The small peak at  $\sim$ 180 ppm in the (OA)<sub>2</sub>O spectrum is due to the presence of an H–OA impurity in the commercial sample. See Figure S6 (Supporting Information) for the full spectrum.

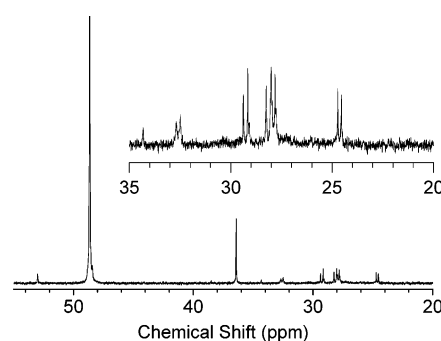


**Figure 3.** <sup>31</sup>P NMR spectrum of a CdSe synthesis in TOPO. The crude reaction mixture was dissolved in CDCl<sub>3</sub>. The inset shows a magnified view of the 20–35 ppm range of the spectrum. The peak for TOPO is at  $\delta$  = 48.7 ppm and that for TOPSe at  $\delta$  = 36.3 ppm.

Aliquots from reactions of Cd–ODPA with TOPSe or TBPS<sub>e</sub> in TOPO show the disappearance of TOPSe and the appearance of <sup>31</sup>P NMR resonances in the range of  $\delta$  = 10–33 ppm. Immediately after injection of TOPSe into a hot mixture of TOPO and Cd–ODPA, several multiplets appear in the <sup>31</sup>P NMR spectrum at  $\delta$  = 32, 29, 28, and 24 ppm (Figure 3). At longer reaction times, additional multiplets could be observed

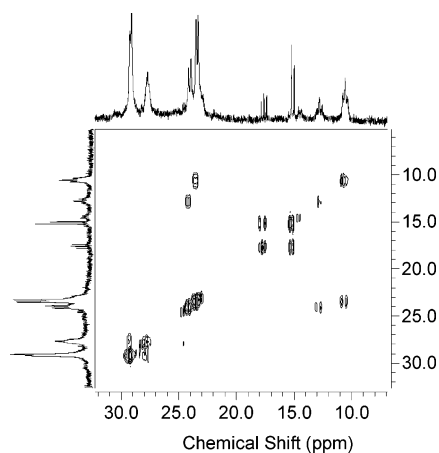


**Figure 4.**  $^{31}\text{P}$ – $^{31}\text{P}$  COSY spectrum of a CdSe synthesis. Peaks of TOPO and TOPSe give no cross-peak and are not shown. The crude reaction mixture was dissolved in  $\text{CDCl}_3$  and flame sealed in an NMR tube under Ar.

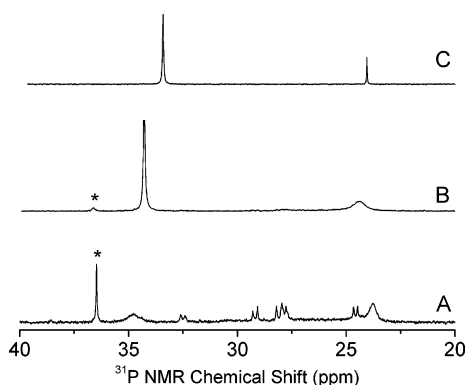


**Figure 5.** Effect of added water on the  $^{31}\text{P}$  NMR spectrum of a TOPSe and Cd–ODPA reaction mixture in TOPO: (A) before and (B) after addition of water to the reaction. (C)  $^{31}\text{P}$  NMR of a 2:1 (w/w) mixture of TOPO and  $\text{H}_2$ –ODPA. An asterisk indicates the TOPSe peak.

in the range of  $\delta = 10$ – $23$  ppm.  $^{31}\text{P}$  homonuclear correlation spectroscopy (COSY) shows that the splitting pattern of these peaks can be explained by  $^{31}\text{P}$ – $^{31}\text{P}$  through-bond coupling ( $J(^{31}\text{P}$ – $^{31}\text{P}) = 35$ – $38$  Hz) (Figure 4). The chemical shift and magnitude of the coupling constants are in the range of reported values for other anhydrides of phosphonic acids ( $\delta = 20$ – $30$  ppm and  $^2J(^{31}\text{P}$ – $^{31}\text{P}) = 25$ – $49$  Hz, for pyrophosphonic acid<sup>38</sup> and tris(*tert*-butyl)triphosphonic acid<sup>39</sup>), suggesting similar anhydride linkages may explain the coupling patterns observed in our spectra. Further confirmation of an anhydride linkage being responsible for the multiplets was provided by addition of water to the reaction mixture at the reaction temperature. Upon addition of water, the multiplets in the  $^{31}\text{P}$  NMR spectrum were immediately replaced by two peaks at  $\delta = 34$  and  $24$  ppm, which are in the range of the resonances observed for  $\text{H}_2$ –ODPA in the presence of TOPO (Figure 5). In addition, the  $^1\text{H}$  NMR showed an increase in the amount of the acid proton.

To further clarify the role of water in the synthesis of CdSe in TOPO, control experiments were carried out by adding water (100 mg) to the reaction after the second degassing but before the TOPSe injection. After injection aliquots of this reaction

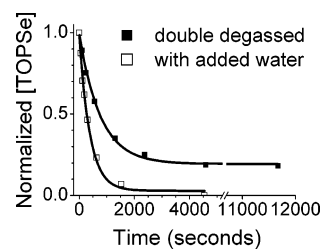


**Figure 6.** Single-exponential fits to the disappearance of TOPSe in the presence of Cd–ODPA in TOPO (Cd–ODPA and TOPSe in TOPO at  $260$  °C). For the reactions with added water, 100 mg of water was added to the flask at  $100$  °C via a syringe after the second degassing but before TOPSe injection.

**Table 3.** Exponential Fits to the Disappearance of Phosphine Chalcogenide<sup>a</sup>

material	precursor	solvent (T, °C)	$k_{\text{obs}} \times 10^3$ (s <sup>-1</sup> )	conversion (%)	note	
1	CdSe	Cd–ODPA/TOPSe	TOPO (290)	$1.7 \pm 0.4$	84	<i>b</i>
2	CdSe	Cd–ODPA/TOPSe	TOPO (260)	$1.30 \pm 0.08$	82	<i>c</i>
3	CdS	Cd–ODPA/TOPS	TOPO (290)	$0.90 \pm 0.54$	30	<i>d</i>
4	CdSe	Cd–OA/TOPSe	$\text{C}_9\text{D}_{20}$ (117)	$1.51 \pm 0.04$	65	<i>e</i>
5	CdSe	Cd–OA/TBPSe	$\text{C}_{10}\text{D}_{22}$ (127)	$2.57 \pm 0.13$	68	<i>e</i>
6	CdSe	Cd–OA/ <i>i</i> -TPPSe	$\text{C}_9\text{D}_{20}$ (127)	0	0	<i>f</i>
7	ZnSe	Zn–ODPA/TOPSe	TOPO (290)	0	0	<i>g</i>
8		$\text{H}_2$ –ODPA/TOPSe	TOPO (290)		15	<i>h</i>

<sup>a</sup> Conversions were calculated using either the amount of TOPSe injected and [TOPSe] of the last aliquot (TOPO-based synthesis) or the fitting results (in situ studies). The reported error in  $k_{\text{obs}}$  is the uncertainty from the fit to a single exponential. <sup>b</sup> Doubly degassed. <sup>c</sup> Mixture of TOPSe (0.70 g) and toluene (0.30 g) was injected at  $320$  °C. <sup>d</sup> Doubly degassed. <sup>e</sup> Mixture of TOPS (0.65 g) and toluene (0.30 g) was injected at  $320$  °C. <sup>f</sup> In situ NMR monitoring. <sup>g</sup> In situ NMR monitoring, reaction time 20 min. <sup>h</sup> Doubly degassed, reaction time 100 min. <sup>h</sup> Reaction time 4 h.

show the appearance of  $^{31}\text{P}$  multiplets at  $\delta = 20$ – $30$  ppm that are replaced by two peaks at  $\delta = 34$  and  $24$  ppm at longer times ( $\sim 1$  h). To confirm that the added water is indeed accessible to the TOPO solution at the reaction temperature, we also carried out a control experiment in which  $\text{H}_2^{18}\text{O}$  (Isotech, 95%  $^{18}\text{O}$ ) was injected into a mixture of TOPO and Cd–ODPA at  $290$  °C. Both FAB-MS and  $^{31}\text{P}$  NMR showed rapid formation of  $^{18}\text{O}$ -substituted TOPO (Figure S10, Supporting Information), which is consistent with an oxygen exchange reaction between  $\text{H}_2^{18}\text{O}$  and TOPO.<sup>40</sup>

**Kinetics of Phosphine Chalcogenide Cleavage.** Reaction kinetics of the CdSe and CdS syntheses were studied by following the concentration of phosphine chalcogenide using  $^{31}\text{P}$  NMR spectroscopy. The decay of phosphine chalcogenide can be fit to a single-exponential decay (Figure 6) and the corresponding  $k_{\text{obs}}$  extracted from the fit (Table 3).<sup>41</sup> The cleavage rates of phosphine chalcogenides increase in the order  $\text{S} < \text{Se} < \text{Te}$  and  $\text{Zn} < \text{Cd}$  by comparing their respective  $k_{\text{obs}}$  or conversion vs time. It was also observed that Cd–OA reacts more rapidly than does Cd–ODPA and both TBPSe and TOPSe are much more reactive than the sterically hindered *i*-TPPSe. A control reaction showed that, in the absence of Cd–OA or Cd–ODPA, TOPSe still decomposed in a mixture of TOPO and  $\text{H}_2$ –ODPA at  $290$  °C (Table 3, entry 8; also see the Supporting Information), although at a rate 2 orders of magnitude slower than in the presence of Cd–OA or Cd–

(38) Ohms, G.; Grossmann, G.; Schwab, B.; Schiefer, H. *Phosphorus, Sulfur Silicon Relat. Elem.* **1992**, *68*, 77–89.

(39) Diemert, K.; Kuchen, W.; Poll, W.; Sandt, F. *Eur. J. Inorg. Chem.* **1998**, 361–366.

(40) Denney, D. B.; Tsois, A. K.; Mislow, K. *J. Am. Chem. Soc.* **1964**, *86*, 4486–4487.

(41) Single-exponential decay of TOPSe was also observed when  $\text{CdMe}_2$  was used as the cadmium precursor in the CdSe synthesis in TOPO (Figure S11, Supporting Information).

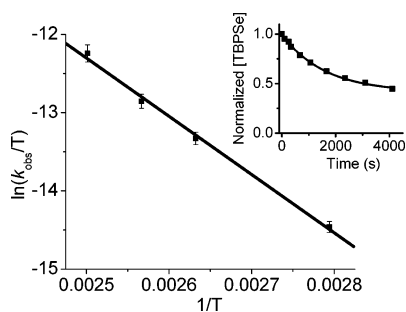


**Figure 7.** Eyring plot of TBPSe reaction with Cd–OA in *n*-decane-*d*<sub>22</sub>. The reactions were carried out at 358, 380, 390, and 400 K. *T* = temperature (Kelvin). The inset shows a representative single-exponential fit to the integrated TBPSe resonance at 380 K.

ODPA. Activation parameters for TBPSe decay in the presence of Cd–OA were determined from the temperature dependence of the exponential fits to the decay curve ( $\Delta H^\ddagger = 62.0 \pm 2.8$  kJ·mol<sup>-1</sup>,  $\Delta S^\ddagger = -145 \pm 8$  J·mol<sup>-1</sup>·K<sup>-1</sup>, Figure 7; also see the Supporting Information).

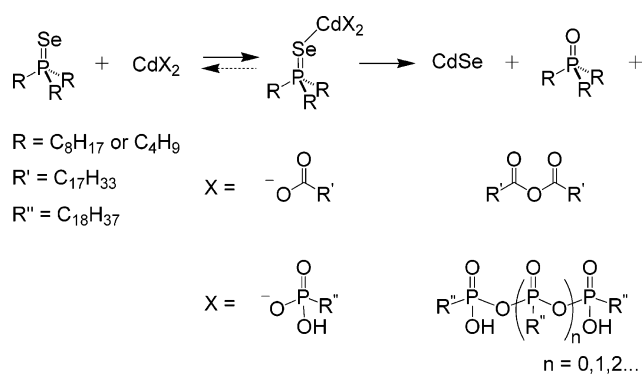
For the reactions carried out in TOPO under anhydrous conditions, the conversion of the trialkylphosphine chalcogenide approaches partial conversion (~80%) even though Cd was used in excess (~10%) in these reactions.<sup>25</sup> The conversion of TBPSe is even lower (~70%) when reacted with Cd–OA in a noncoordinating solvent at relatively low temperature (360–400 K). Interestingly, if water was added to the TOPO-based reaction, either before or after the injection of TOPSe, the conversion of TOPSe could be increased to almost 100% (Figure 6).

## Discussion

Previous studies on the formation of group II–VI nanocrystals have focused on the role of surfactant molecules in controlling particle growth by binding to the nanocrystal surface. In this study we have gathered evidence that phosphonic and carboxylic acids are also reactants responsible for the conversion of precursor molecules to the metal chalcogenide. In particular, the conversion of TOPSe and TBPSe to their corresponding phosphine oxides is linked to the formation of anhydrides of *n*-octadecylphosphonic acid and oleic acid, suggesting that phosphonic and carboxylic acids are responsible for cleavage of the phosphorus–chalcogen double bond. A partial mechanism for this transformation is shown in Scheme 1.

**Cadmium Precursors.** Observations in this study as well as those by Peng and co-workers indicate that the reaction between CdO and phosphonic acids produces a phosphonic acid complex of cadmium and 1 equiv of water.<sup>5,25,42</sup> The broad <sup>31</sup>P NMR resonance, high viscosity, and low solubility of Cd–ODPA in CDCl<sub>3</sub> support the idea that the cadmium precursor of this synthesis is a coordination polymer. Single-crystal X-ray studies of Cd(O<sub>3</sub>PCH<sub>3</sub>)·H<sub>2</sub>O and Cd(O<sub>3</sub>PC<sub>6</sub>H<sub>5</sub>)·H<sub>2</sub>O provide structurally characterized examples of this type of coordination polymer that is composed of layers of cadmium ions bridged together by phosphonate groups.<sup>43</sup> Unlike Cd–ODPA, Cd–OA is soluble in CDCl<sub>3</sub> and gives sharp <sup>1</sup>H and <sup>13</sup>C NMR resonances, which does not, however, rule out the possibility that this compound also forms a similar coordination polymer or oligomeric

**Scheme 1.** Proposed Reaction Pathway for Precursor Conversion<sup>a</sup>



<sup>a</sup> The X substituent may change as the reaction proceeds, which will change the identity of the soluble cadmium ions as well as the TOPE–CdX<sub>2</sub> complex. See the discussion in the text.

structure. Single-crystal structures of cadmium acetate and self-assembled monolayers of other long-chain carboxylic acid complexes of cadmium support the notion that Cd–OA may also be a coordination polymer under our conditions despite its sharp NMR resonances.<sup>44</sup> The low solubility of Zn–OA in CDCl<sub>3</sub> may be due to a polymeric structure in this case.

**Reaction Products.** In reactions where oleic acid was used as a surfactant molecule, the formation of group II–VI nanocrystals was accompanied by the formation of trialkylphosphine oxides and (OA)<sub>2</sub>O (Table 2). Clear identification of the trialkylphosphine oxide and oleic acid anhydride products was possible by comparing their respective <sup>31</sup>P and <sup>13</sup>C NMR spectra with those of authentic samples (Figures 1 and 2). Monitoring the <sup>31</sup>P and <sup>1</sup>H NMR spectra of our reaction mixtures showed that the disappearance of the trialkylphosphine selenide and the appearance of its corresponding phosphine oxide match the extent of (OA)<sub>2</sub>O formation (Figure 1). These observations suggest that these molecules are derived from one another according to the stoichiometry in Scheme 1.

On the other hand, the products from nanocrystal syntheses performed in TOPO and H<sub>2</sub>–ODPA were more difficult to characterize. The formation of trialkylphosphine oxide from the corresponding trialkylphosphine selenide, for instance, could not be unambiguously characterized with <sup>31</sup>P NMR spectroscopy due to overlap with the TOPO solvent. Instead, FAB–MS was used to identify the TBPO product of TBPSe cleavage (Figure S5). <sup>31</sup>P NMR spectra of the reaction mixtures show the appearance of several multiplets, not observed in reactions using oleic acid, whose intensities are dependent on the extent of reaction and the presence of water. Two observations lead us to believe these resonances are from anhydrides of ODPA. <sup>31</sup>P–<sup>31</sup>P COSY showed that their multiplicity arises from phosphorus–phosphorus through-bond coupling with coupling constants similar to other known examples of phosphonic acid anhydrides. Further, the multiplets could be converted to H<sub>2</sub>–ODPA upon hydrolysis (Figure 5). The appearance of additional <sup>31</sup>P multiplets at longer reaction times may be the result of deoxygenation of the phosphonic acid anhydride product producing multiple anhydride linkages in an oligomeric structure like the one drawn in Scheme 1 (*n* > 0). Alternatively these resonances may derive from one phosphonic acid anhydride trimer (*n* = 1) in different coordination environments. Although more

(42) Carbone, L.; Kudera, S.; Carlino, E.; Parak, W. J.; Giannini, C.; Cingolani, R.; Manna, L. *J. Am. Chem. Soc.* **2006**, *128*, 748–755.

(43) Cao, G.; Lynch, V. M.; Yacullo, L. N. *Chem. Mater.* **1993**, *5*, 1000–1006.

(44) Harrison, W.; Trotter, J. *J. Chem. Soc., Dalton Trans.* **1972**, 956–960.



work is needed to assign these multiplets, an anhydride linkage reasonably explains the  $^{31}\text{P}$ – $^{31}\text{P}$  coupling observed in the spectrum of the reaction products and the reaction of this species with water.

The formation of  $(\text{OA})_2\text{O}$  and octadecylphosphonic acid anhydrides under anhydrous conditions requires that 2 equiv of octadecylphosphonate and oleate are consumed in the cleavage reaction. In the presence of water, however, the anhydride product can undergo subsequent hydrolysis, regenerating the phosphonic or carboxylic acid surfactant. CdSe syntheses conducted in TOPO with added water still, however, produce  $(\text{ODPA})_{n+1}\text{O}_n$ , which, at longer times, revert back to  $\text{H}_2$ –ODPA. These observations suggest that at 260–290 °C the concentration of water in the reaction mixture is not high enough to compete with  $\text{H}_2$ –ODPA for cleavage of the TOPSe molecule.<sup>45,46</sup>

**TOPSe–Cd<sup>2+</sup> Coordination.** The polymeric structure of Cd–ODPA is likely due to the Lewis acidity of the Cd<sup>2+</sup> ion, which binds to adjacent phosphonate oxygens in an attempt to fill its coordination sphere. On this basis it is not surprising that the electron-rich selenium atom of trialkylphosphine selenide would bind to Cd<sup>2+</sup>. In fact, alkyl- and arylphosphine chalcogenides have been shown to coordinate to a large number of transition-metal ions, including Cd<sup>2+</sup> and Zn<sup>2+</sup>, resulting in a weakening of the P=E (E = S, Se, Te) double bond.<sup>47–49</sup> Our  $^{31}\text{P}$  NMR studies show the resonance of TOPSe shifts to higher  $\delta$  along with a decreased  $^1J(^{31}\text{P}$ – $^{77}\text{Se})$  in  $\text{CDCl}_3$  solutions of cadmium 2-ethylhexanoate, suggesting the formation of a TOPSe–Cd<sup>2+</sup> complex (Table 1).<sup>50–52</sup> These spectroscopic changes were not observed, however, when TOPSe was combined with Cd–ODPA, supporting a weaker coordination of TOPSe to Cd–ODPA than Cd–OA. This difference may be due, in part, to a more coordinatively unsaturated cadmium center in Cd–OA and offers an explanation of the faster TOPE cleavage by Cd–OA.

**Cleavage of the P=E Bond.** A number of experimental observations suggest that the TOPE precursor is converted to cadmium and zinc chalcogenides by a substitution reaction in which a Lewis acidic cadmium or zinc center activates TOPE to nucleophilic attack by phosphonate or carboxylate (Figure 8).<sup>53,54</sup> First, TOPSe cleavage proceeds at a rate 2 orders of magnitude faster in the presence of Cd–ODPA and TOPO than  $\text{H}_2$ –ODPA and TOPO alone, providing support for the Lewis acid activation step.<sup>55</sup> Second, the large and negative entropy

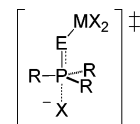


**Figure 8.** Hypothetical transition structure for TOPE cleavage.

of activation extrapolated from the Eyring plot in Figure 7 suggests that the steps leading to TBPSe cleavage in the presence of the Lewis acidic cadmium center involve the association of two or more molecules. This suggestion is made tentatively, however, since the single-exponential fits to TOPSe decay are not likely to result from first-order kinetics. This is especially true because the reactions approach partial conversion and were not run under pseudo-first-order conditions. Third, the sterically hindered *i*-TPPSe reacts with Cd–OA much slower than does TBPSe, which argues against unimolecular decomposition of the P=Se fragment. Finally, formation of phosphine oxides via cleavage of P=X double bonds frequently involves two steps where an electrophile is first bound to X followed by addition of an oxygen nucleophile to the phosphorus center. Previous studies of alkyl- and arylphosphine selenides and sulfides (X = Se, S) have shown that conversion to the corresponding phosphine oxide under nonoxidizing conditions can proceed via a Lewis acid-catalyzed substitution mechanism. In these studies triphenylphosphine selenide or sulfide, when activated by trifluoroacetic anhydride, undergoes attack by nucleophiles as weak as trifluoroacetate, yielding triphenylphosphine oxide.<sup>56,57</sup> In a similar vein, the accepted mechanisms for the cleavage of Wittig (X=CR<sub>2</sub>) and aza-Wittig (X=NR) reagents involve addition to the phosphorus center upon reaction of an electrophile with the nucleophilic terminus of the P=X double bond.<sup>58</sup> All these points argue for a similar cleavage reaction under our conditions where nucleophilic addition to the phosphorus center proceeds upon Lewis acid activation of TOPE by the cadmium or zinc precursor.

**Role of the Surfactant as a Reagent.** Surfactants such as  $\text{H}_2$ –ODPA and H–OA have been extensively used to control the growth of nanocrystals. Their major role has long been believed to be the selective adhesion to the nanocrystal surface,<sup>3,25</sup> as well as controlling monomer solubility.<sup>7,28,29</sup> However, our results show that  $\text{H}_2$ –ODPA and H–OA are ultimately responsible for cleavage of the P=Se bond. Hence, changing the concentration of these surfactants<sup>3,4,25</sup> will likely change the TOPE cleavage kinetics in addition to the binding of surfactants to the nanocrystal surface.<sup>59</sup> This is especially important given that the alkylphosphine chalcogenide cleavage is likely the reaction leading to the formation of semiconductor monomers, and hence, the rate of this cleavage will influence particle nucleation and growth.

The generation of multiple anhydride linkages indicates that both ODPA and its anhydride can cleave the P=Se bond. This change in the cleavage agent over the course of reactions

(45) The slow hydrolysis rate also suggests that most of the added water does not dissolve in the reaction mixture at 260–290 °C.

(46) Cd–ODPA showed increased reactivity toward TOPS cleavage with added water, suggesting that water may contribute to the cleavage mechanism in that case. See Figure S12, Supporting Information.

(47) Karayannis, N. M.; Mikulski, C. M.; Pytlewski, L. L. *Inorg. Chim. Acta, Rev.* **1971**, *5*, 69–105.

(48) Lobana, T. S.; Gupta, T. R.; Sandhu, S. S. *Polyhedron* **1982**, *1*, 781–783.

(49) Lobana, T. S. In *The chemistry of organophosphorous compounds*; Hartley, F. R., Ed.; John Wiley & Sons: New York, 1992; Vol. 2, p 487.

(50) Grim, S. O.; Walton, E. D.; Satek, L. C. *Can. J. Chem.* **1980**, *58*, 1476–1479.

(51) Dean, P. A. W.; Polensek, L. *Can. J. Chem.* **1980**, *58*, 1627–1632.

(52) Dean, P. A. W.; Hughes, M. K. *Can. J. Chem.* **1980**, *58*, 180–190.

(53) Whether the nucleophile is free in solution as shown in Figure 8 or bound to cadmium is unknown. The transition structure drawn was chosen for the sake of simplicity.

(54) Quantitation of the CdSe nanocrystal produced upon TOPSe cleavage in TOPO/Cd–ODPA by monitoring the size-independent particle absorption at 350 nm (Leatherdale, C. A.; Woo, W. K.; Mikulec, F. V.; Bawendi, M. G. *J. Phys. Chem. B* **2002**, *106*, 7619–7622) and  $^{31}\text{P}$  NMR spectra of reaction aliquots showed the extent of TOPSe cleavage matches the appearance of CdSe: Owen, J. S.; Liu, H. T.; Alivisatos, A. P. Manuscript in preparation.

(55) Other studies have also shown that phosphine sulfide and selenide could be converted to phosphine oxide by organic Lewis acid like trifluoroacetic acid anhydride. See ref 57.

(56) Chen, C. H.; Brighty, K. E. *Tetrahedron Lett.* **1980**, *21*, 4421–4424.

(57) Helinski, J.; Skrzypczynski, Z.; Wasiak, J.; Michalski, J. *Tetrahedron Lett.* **1990**, *31*, 4081–4084.

(58) Smith, M. B.; March, J. *March's Advanced Organic Chemistry: Reactions, Mechanisms, and Structure*, 5th ed.; Wiley-Interscience: New York, 2001; p 1231.

(59) Studies in our laboratory to identify the dependence of the reaction kinetics on phosphonic acid are under way: Owen, J. S.; Liu, H. T.; Alivisatos, A. P. Manuscript in preparation.

conducted with  $\text{H}_2\text{-ODPA}$  indicates more reaction pathways than shown in Scheme 1, especially at longer reaction times. In particular changes to the soluble cadmium precursor and the surfactant molecules that bind it undoubtedly impact the mechanistic details of the TOPE binding and cleavage. Several observations highlight this point. Added water leads to an increase in TOPSe conversion suggesting that  $(\text{ODPA})_{n+1}\text{O}_n$  may inhibit the cleavage reaction by binding to the cadmium precursor or by replacing its ODPA ligands.<sup>60,61</sup> We also observe partial conversion in CdSe syntheses using Cd-OA and TBPSe in a noncoordinating solvent which cannot be explained by the appearance of the anhydride product since  $(\text{OA})_2\text{O}$  should bind cadmium only weakly. The limited yield in this case and in reactions conducted with  $\text{H}_2\text{-ODPA}$  may arise from the buildup of dissolved cadmium selenide that deactivates the soluble cadmium precursor and inhibits TOPSe binding and cleavage. Additionally, the reactivity of  $\text{Cd}(\text{OA})_2$  may be decreased by coordination of the phosphine oxide product.<sup>49,62</sup>

Finally, our results argue against other proposals for the mechanism of ME ( $\text{M} = \text{Cd}, \text{Zn}$ ;  $\text{E} = \text{S}, \text{Se}, \text{Te}$ ) formation from trialkylphosphine chalcogenides and phosphonic and oleic acid complexes of cadmium and zinc. In particular, pathways involving formation of atomic cadmium, zinc, or chalcogen do not adequately explain our results. These reactions can be expected to display positive entropies of activation since two or more molecules should be generated in the homolysis reaction. Neither do such pathways easily explain the clean formation of phosphonic acid anhydrides or oleic acid anhydride and trialkylphosphine oxide observed in this study.

## Conclusion

We have shown that TOPE (or TBPE;  $\text{E} = \text{S}, \text{Se}, \text{Te}$ ) reacts with Cd and Zn precursors (oleate or alkylphosphonate) to produce ME ( $\text{M} = \text{Cd}, \text{Zn}$ ) nanocrystals, TOPO (or TBPO), and oleic or phosphonic acid anhydrides. We propose a Lewis acid-activated substitution mechanism for this reaction on the basis of the several points: (1) TOPSe undergoes cleavage more rapidly in the presence of Cd-ODPA than  $\text{H}_2\text{-ODPA}$  alone, (2) previous mechanistic studies of  $\text{P}=\text{X}$  cleavage, (3) the concurrent formation of TBPO or TOPO and  $(\text{OA})_2\text{O}$  or  $(\text{ODPA})_{n+1}\text{O}_n$ , and (4) kinetics evidence for the association of two or more molecules in the steps leading to  $\text{P}=\text{Se}$  cleavage. TBPO and oleic acid anhydride were also observed in the synthesis of CdS, CdTe, ZnS, ZnSe, and ZnTe nanocrystals using TBPE and M-OA, suggesting a common cleavage reaction when phosphine chalcogenides are used as a precursor in combination with cadmium and zinc phosphonates and

oleates.<sup>63,64–66</sup> Our results demonstrate the importance of surfactant molecules as reagents in the conversion of precursor molecules to group II–VI semiconductor materials, which we hope will lead to a better understanding of particle nucleation and growth kinetics. Continuing work in our laboratory focuses on how surfactant molecules control phosphine chalcogenide cleavage kinetics and thus influence particle nucleation. We hope these results will prove useful in the design of new synthetic methodologies.<sup>67</sup>

**Note Added in Proof.** A study by Bawendi and co-workers on the mechanism of PbSe formation supports a similar mechanism in this case.<sup>68</sup>

**Acknowledgment.** This work was supported by the Director, Office of Science, Office of Basic Energy Sciences, Materials Sciences and Engineering Division, of the U.S. Department of Energy under Contract No. DE-AC02-05CH11231. J.S.O. acknowledges the donors of the American Chemical Society Petroleum Research Fund for their partial support of this research. We thank Professor Robert G. Bergman and Professor T. Don Tilley for helpful discussions and Dr. Herman van Halbeek for assistance with the 2D NMR experiment.

**Supporting Information Available:** <sup>31</sup>P NMR analysis of the impurities in TOPO, stability of TOPSe and TBPSe in air, deconvolution of the TOPO and TOPS resonances using MestRec, accuracy of the NMR method, synthesis and characterization of TBPE, TOPE ( $\text{E} = \text{S}, \text{Se}, \text{Te}$ ), and *i*-TPPSe, Karl Fischer titration methods, FAB-MS spectrum of CdSe synthesis using Cd-OA and TBPSe in *n*-decane-*d*<sub>22</sub>, FAB-MS spectrum of CdSe synthesis using TBPSe and Cd-ODPA in TOPO, full spectrum of Figure 2, product characterization of the synthesis of CdS, CdTe, ZnS, ZnSe, and ZnTe in a noncoordinating solvent, transmission electron micrograph of CdSe and CdS nanocrystals, UV-vis spectra of CdSe nanocrystals, experimental procedure of the TOPO- $\text{H}_2^{18}\text{O}$  isotope exchange reaction, experimental procedure of activation parameter measurement, reaction kinetics of CdSe synthesis in TOPO using  $\text{CdMe}_2$  as the cadmium precursor, decomposition of TOPSe in TOPO/ $\text{H}_2\text{-ODPA}$  in the absence of  $\text{Cd}^{2+}$ , and reaction kinetics of CdS synthesis in TOPO. This material is available free of charge via the Internet at <http://pubs.acs.org>.

JA0656696

(60) Spanhel, L.; Haase, M.; Weller, H.; Henglein, A. *J. Am. Chem. Soc.* **1987**, *109*, 5649–5655.

(61) We note that a cadmium center coordinated by the more acidic anhydride of ODPA is likely to bind and activate TOPSe to a greater extent, but may also be a weaker nucleophile in the cleavage step.

(62) Bond, A. M.; Colton, R.; Ebner, J.; Ellis, S. R. *Inorg. Chem.* **1989**, *28*, 4509–4516.

(63) We note that, in the absence of acid surfactant, some precursors, such as phosphine telluride, could react differently. See refs 64–66.

(64) Stuczynski, S. M.; Kwon, Y. U.; Steigerwald, M. L. *J. Organomet. Chem.* **1993**, *449*, 167–172.

(65) Steigerwald, M. L.; Siegrist, T.; Stuczynski, S. M.; Kwon, Y. U. *J. Am. Chem. Soc.* **1992**, *114*, 3155–3156.

(66) Steigerwald, M. L.; Rice, C. E. *J. Am. Chem. Soc.* **1988**, *110*, 4228–4231.

(67) Narayanaswamy, A.; Xu, H.; Pradhan, N.; Kim, M.; Peng, X. *J. Am. Chem. Soc.* **2006**, *128*, 10310–10319.

(68) Steckel, J. S.; Yen, B. K. H.; Oertel, D. C.; Bawendi, M. G. *J. Am. Chem. Soc.*, in press.